Soft Matter

RSC Publishing

PAPER

View Article Online
View Journal | View Issue

Self-healing polyacrylic acid hydrogels†

Cite this: *Soft Matter*, 2013, **9**, 10287

Umit Gulyuz and Oguz Okay*

pH responsive physical gels were prepared by micellar copolymerization of acrylic acid with 2 mol% stearyl methacrylate (C18) in a solution of worm-like sodium dodecyl sulfate micelles. The physical gels are insoluble in water and exhibit time-dependent dynamic moduli, high Young's modulus (6–53 kPa), high fracture stress (41–173 kPa), high elongation ratios at break (1800–5000%), and self-healing, as evidenced by rheological and mechanical measurements. Cyclic elongation tests show significant hysteresis due to the existence of reversibly breakable bonds (up to 25%) within the gel network. As the polymer concentration is increased, both the lifetime of hydrophobic associations and the mechanical strength of gels increase while the elongation ratio at break decreases. As compared to the polyacrylamide gels formed under identical conditions, the present hydrogels exhibit a much stronger self-healing effect, which is attributed to the cooperative hydrogen bonding between the carboxyl groups stabilizing the hydrophobic domains. The efficiency of self-healing significantly increases with increasing temperature due to the decrease of the lifetime of hydrophobic associations.

Received 25th July 2013
Accepted 10th September 2013

DOI: 10.1039/c3sm52015c

www.rsc.org/softmatter

Introduction

Self-healing is one of the most remarkable properties of biological materials such as skin, bones, and wood.[1–3] Autonomous damage repair and resulting healing in such materials often involve an energy dissipation mechanism created by reversible bonds which prevent the fracture of the molecular backbone.[4] Although synthetic hydrogels are very similar to biological tissues, and therefore have been important materials for drug delivery and tissue engineering, they are normally very brittle and lack the ability to self-heal upon damage. Inspired by natural healing processes, different reversible molecular interactions have been used recently to generate self-healing hydrogels, including hydrogen bonding,[5–9] electrostatic interactions,[10–12] molecular recognition,[13–15] metal coordination,[16,17] π–π stacking,[18] dynamic chemical bonds,[19–22] molecular diffusion,[23,24] and hydrophobic associations.[25–28] However, self-healing hydrogels synthesized so far suffer from low mechanical strength which may limit their use in any stress-bearing applications such as artificial cartilages. This mechanical weakness is due to the fact that the self-healing ability of a hydrogel is antagonist to its mechanical strength.[29,30] For instance, decreasing the lifetime of dynamic cross-links increases the efficiency of self-healing due to the favourable chain diffusion across fractured surfaces of hydrogels. In contrast, hydrogels with short-living cross-links necessarily become weak at experimental time scales. Hence, the design of self-healing gels with a good mechanical performance such as a high mechanical strength is crucially important in many existing and potential application areas of soft materials.

Recently, we presented a simple strategy for the production of self-healing hydrogels *via* hydrophobic interactions.[25,29–31] Large hydrophobes such as stearyl methacrylate (C18) or dococyl acrylate could be copolymerized with the hydrophilic monomer acrylamide (AAm) in aqueous surfactant solutions. This was achieved by the addition of salt (NaCl) into the reaction solution.[25] Salt leads to micellar growth and hence solubilisation of large hydrophobes within the grown wormlike surfactant micelles.[25,29] Incorporation of hydrophobic sequences within the hydrophilic polyacrylamide (PAAm) chains *via* the micellar polymerization technique generates strong hydrophobic interactions, which prevent dissolution of the physical gels in water, while the dynamic nature of the junction zones provides homogeneity and self-healing properties.[25,29–31] Since the blocky structure of hydrophobically modified polymers formed by micellar polymerization enhances significantly their associative properties,[32–38] these hydrogels exhibit rapid self-healing at room temperature without the need for any stimulus or healing agent.

We propose that a stronger self-healing in such hydrogels could be achieved by replacing PAAm with a polyacrylic acid (PAAc) backbone that would mediate hydrogen bonding across a rupture in the hydrogel. Although polyelectrolytes such as PAAc are among the most studied polymeric systems, several experimental findings are still poorly described due to the presence of both long-range and short-range interactions.[39–41] Recent studies show an important mechanical hysteresis in chemically

Department of Chemistry, Istanbul Technical University, 34469 Istanbul, Turkey. E-mail: okayo@itu.edu.tr; Fax: +90-2122856386; Tel: +90-2122853156

† Electronic supplementary information (ESI) available: Swelling behavior, temperature dependence of the dynamic moduli, and the effect of urea on the self-healing behavior of PAAc hydrogels. See DOI: 10.1039/c3sm52015c

cross-linked PAAc hydrogels for a range of deformations.[40,41] This is unexpected, given that chemical gels are elastic materials with negligible viscous properties. Since the hysteresis in PAAc hydrogels is much less pronounced in salt solutions,[40] the existence of ionic associations due to electrostatic interactions seems to be responsible for the energy dissipation under strain. It was also shown that the thermal stability of crystalline domains formed by long alkyl side chains is higher in the PAAc backbone than in the PAAm backbone.[42] This was attributed to the cooperative hydrogen bonding between the carboxyl groups stabilizing the crystalline domains.[42,43]

Thus, we hypothesize that large hydrophobic blocks attached to the PAAc backbone would produce mechanically strong self-healing hydrogels due to the presence of hydrophobic associations acting as reversible cross-links stabilized by the cooperative hydrogen bonding between carboxyl groups. Here, we prepared physical PAAc hydrogels by the micellar copolymerization of acrylic acid (AAc) with 2 mol% C18 in aqueous solutions of worm-like sodium dodecylsulfate (SDS) micelles. As will be shown below, replacement of PAAm with PAAc network chains significantly improves the self-healing performance of the hydrogels. The results also show that the healing temperature is an important parameter to generate healing in mechanically strong PAAc hydrogels. Hydrogels healed at 80 °C withstand more than 120 kPa stress at an elongation ratio of 1500%.

Experimental part

Materials

Acrylic acid (AAc, Merck), acrylamide (AAm, Merck), *N*,*N*′-methylenebis(acrylamide) (BAAm, Merck), sodium dodecylsulfate (SDS, Merck), ammonium persulfate (APS, Sigma-Aldrich), sodium pyrosulfite ($Na_2S_2O_5$, Fluka), and NaCl (Merck) were used as received. Commercially available stearyl methacrylate (C18, Aldrich) consists of 65% *n*-octadecyl methacrylate and 35% *n*-hexadecyl methacrylate. Stock solutions were prepared by dissolving 0.8 g APS and 0.19 g $Na_2S_2O_5$ separately in 10 mL of distilled water.

Hydrogel preparation

Micellar copolymerization of AAc with 2 mol% C18 was conducted at 50 °C in the presence of an APS (3.5 mM) – $Na_2S_2O_5$ (1 mM) redox initiator system in SDS–NaCl solutions. NaCl concentration was fixed at 0.5 M, at which the aggregation number of SDS micelles is about 200,[25] as compared to 60 for the minimum spherical SDS micelle. The total monomer concentration C_0 was varied between 15 and 30 w/v%. SDS concentration required for the solubilisation of the hydrophobe in the reaction solution was determined by measuring the transmittance of the solution, as detailed before.[25,29] For C_0 = 15, 20, and 30 w/v%, SDS contents required were 8.5, 10, and 14 w/v%, respectively. The initial pH of the reaction solution was 1.5 so that AAc is mostly protonated. To illustrate the synthetic procedure, we give details of the preparation of hydrogels at C_0 = 15 w/v%. SDS (0.85 g) was dissolved in 8.0 mL of 0.5 M NaCl at 35 °C to obtain a transparent solution. Then, C18 (0.1278 g) was dissolved in this SDS–NaCl solution under stirring for 5 h at 35 °C. After addition and dissolving AAc (1.3722 g) for 30 min, stock solutions of $Na_2S_2O_5$ (100 μL) and finally APS (100 μL) were added to initiate the reaction. A portion of this solution was transferred between the plates of the rheometer to follow the reaction by oscillatory small-strain shear measurements. For the determination of the gel fraction and for the mechanical measurements, the remaining part of the solution was transferred into several plastic syringes of 4.8 mm internal diameter and the polymerization was conducted for one day at 50 °C.

Rheological experiments

Gelation reactions were carried out at 50 °C within the rheometer (Gemini 150 Rheometer system, Bohlin Instruments) equipped with a cone-and-plate geometry with a cone angle of 4° and a diameter of 40 mm. The instrument was equipped with a Peltier device for temperature control. During all rheological measurements, a solvent trap was used to minimize the evaporation. An angular frequency ω of 6.3 rad s^{-1} and a deformation amplitude γ_o of 0.01 were selected to ensure that the oscillatory deformation is within the linear regime. After a reaction time of 2 h, the dynamic moduli of the reaction solutions approached limiting values. Then, frequency-sweep tests were carried out at 25 °C, as described before.[25]

Uniaxial elongation measurements

The measurements were performed on cylindrical hydrogel samples (4.8 mm diameter × 6 cm length) at 23 ± 2 °C on a Zwick Roell test machine using a 10 N load cell under the following conditions: crosshead speed = 5 and 50 mm min^{-1} for elongation ratios $\lambda < 0.15$ and $\lambda > 0.15$, respectively; sample length between jaws = 12 ± 2 mm. The stress was presented by its nominal value σ_{nom}, which is the force per cross-sectional area of the undeformed gel specimen, while the strain is given by λ, the elongation ratio (deformed length/initial length). % Elongation was calculated as $(\lambda - 1) \times 10^2$. The tensile strength and the elongation ratio at break were recorded. The tensile modulus was calculated from the slope of stress-strain curves between elongations of 5% and 15%. Cyclic elongation tests were conducted at a constant crosshead speed of 50 mm min^{-1} to a maximum elongation ratio, followed by retraction to zero force and a waiting time of 10 min, until the next cycle of elongation. For reproducibility, at least six samples were measured for each gel and the results were averaged.

Gel fractions and swelling measurements

Cylindrical hydrogel samples (diameter 4.8 mm, length about 2 cm) were immersed in a large excess of water at 23 ± 2 °C for at least 15 days by replacing water every second or third day to extract any soluble species. The mass *m* of the gel samples was monitored as a function of swelling time by weighing the samples. The relative weight swelling ratio m_{rel} of gels was calculated as $m_{rel} = m/m_0$, where m_0 is the initial mass of the gel sample. Then, the equilibrium swollen gel samples with a relative mass $m_{rel,eq}$ were taken out of water and freeze dried.

The gel fraction W_g, that is, the conversion of monomers to the water-insoluble polymer (mass of water-insoluble polymer/initial mass of the monomer), was calculated from the mass of the dry, extracted polymer network and from the comonomer feed. Swelling measurements were also conducted in aqueous solutions of various pH values between 2 and 11 adjusted by adding either HCl or NaOH solutions.

Results and discussion

Self-healing hydrogels were prepared by the micellar copolymerization of AAc with 2 mol% C18 at 50 °C and at various initial monomer concentrations C_0 between 15 and 30 w/v%. Gelation reactions were monitored by rheometry using oscillatory deformation tests. Fig. 1A shows the elastic modulus G', the viscous modulus G'', and the loss factor tan δ ($=G''/G'$) plotted against the reaction time at various C_0. In the absence of the hydrophobe (not shown), the micellar polymerization of AAc produces a semi-dilute solution of PAAc (Fig. S1 and 2†). In the presence of C18, the dynamic moduli of the reaction system increase while tan δ decreases rapidly as the reaction proceeds and then approach plateau values after 1–2 h (Fig. 1A). The decrease of tan δ below unity demonstrates gel formation by incorporation of the hydrophobic blocks into the PAAc chains and formation of intermolecular associations. Increasing C_0 from 15 to 30 w/v% also increases the final elastic modulus from 1.6 to 20 kPa while the loss factor decreases from 0.5 to 0.2 indicating increasing elasticity of the physical gels.

Fig. 1B shows the frequency dependencies of G' and G'' at 25 °C for the gels after a reaction time of 2 h. For comparison, the data obtained from a chemically cross-linked PAAc gel formed at $C_0 = 15$ w/v% are also shown in the figure. In contrast to the chemical PAAc gel that exhibits a frequency-independent elastic modulus, the physical gels exhibit frequency-dependent dynamic moduli indicating the temporary nature of the hydrophobic associations having lifetimes on the order of seconds to milliseconds. Over two decades of frequencies corresponding to time scales between 10^{-1} and 10^{1} s, G' exhibits a power-law behavior, $G' \propto \omega''$, with an exponent $n = 0.32$, 0.16, and 0.14 for $C_0 = 15$, 20, and 30 w/v%, respectively. Thus, as the AAc concentration is increased, the modulus becomes less frequency-dependent, that is, the lifetime of the hydrophobic associations increases.

Gelation reactions were also conducted in plastic syringes at 50 °C for one day to obtain rod-shaped gel samples for the gel fraction, swelling and mechanical measurements. Physical gels formed at $C_0 = 15\%$ were too weak in the equilibrium swollen state in water and disintegrated into small gel particles after about 2 weeks. In contrast, those formed at $C_0 = 20$ and 30% were stable and exhibited equilibrium swelling ratios ($m_{rel,eq}$) of 500 ± 70 and 80 ± 30, respectively. The gel fraction W_g, *i.e.*, the mass of water-insoluble polymer obtained from one gram of AAc–C18 mixture in the feed, was 1.00 ± 0.03 and 0.83 ± 0.01 for $C_0 = 20$ and 30%, respectively. This reveals that, although the gels exhibit a large swelling ratio in water because of the osmotic pressure of AAc counterions, the hydrophobic associations are so strong that they are not destroyed during the expansion of the gel network in water. Swelling measurements conducted in aqueous solutions of various pH values between 2 and 11 showed typical behaviour of chemical PAAc hydrogels, *i.e.*, increasing degree of swelling with the increase in pH up to 7 and then levelling off between pH 7 and 11 (Fig. S3†).

Cylindrical hydrogel samples after a reaction time of 24 h were also subjected to uniaxial elongation tests. Young's modulus E, the fracture stress σ_f, and the elongation ratio λ_f at break of the physical gels are given in Table 1. Fig. 2A represents typical tensile stress–strain data of the physical gels as the dependence of the nominal stress σ_{nom} on the elongation ratio λ. At $C_0 = 15\%$, the gel withstands 41 ± 11 kPa stress while the fracture stress further increases up to 173 ± 33 kPa as C_0 is increased. The elongation ratio at break of the hydrogels is between 19 and 51 (1800–5000% elongations), which is a decreasing function of C_0.

Cyclic mechanical testing is a powerful tool to understand the nature of cross-links in the physical gels.[40] The dashed rectangular area in Fig. 2A shows the region where cyclic elongation tests were conducted, while Fig. 2B is a zoom-in to this area. The tests were carried out by first elongating the gel

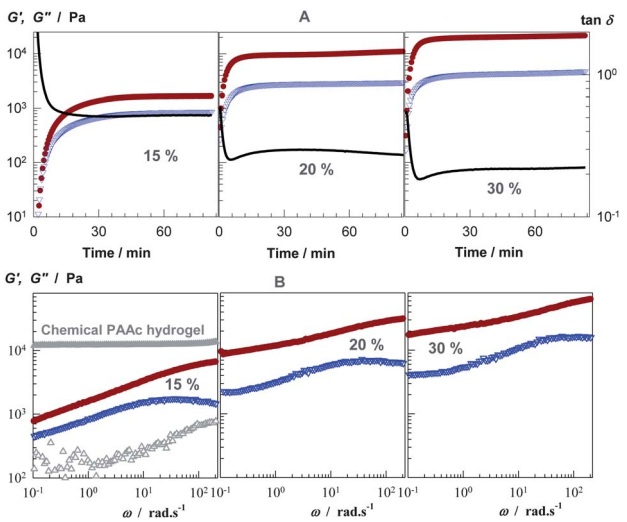

Fig. 1 (A) G' (●), G'' (▼) and tan δ (lines) during the micellar copolymerization of AAc and C18 (2 mol%) at 50 °C shown as a function of the reaction time. $\omega = 6.28$ rad s^{-1}. $\gamma_o = 0.01$. (B) G' (●) and G'' (▼) of PAAc gels formed after a reaction time of 2 h shown as a function of frequency ω. Temperature = 25 °C. The concentration of AAc (in w/v%) in the feed is indicated. For comparison, G' (▲) and G'' (△) of a chemically cross-linked PAAc hydrogel are also given. The chemical gel was prepared at $C_0 = 15$ w/v% using the BAAm cross-linker (molar ratio of BAAm to AAc = 1/50).

Table 1 Characteristic data for PAAc hydrogels

C_0 w/v%	E^a kPa	σ_f^b kPa	λ_f^c	ν_e^d mol m^{-3}
15	6 (1)	41 (11)	51 (8)	0.81 (0.14)
20	18 (2)	123 (5)	29 (1)	2.4 (0.3)
30	53 (3)	173 (33)	19 (1)	7.2 (0.4)

[a] Young's modulus. [b] Fracture stress. [c] Elongation ratio at break. [d] Apparent cross-link density. (standard deviations in parentheses.)

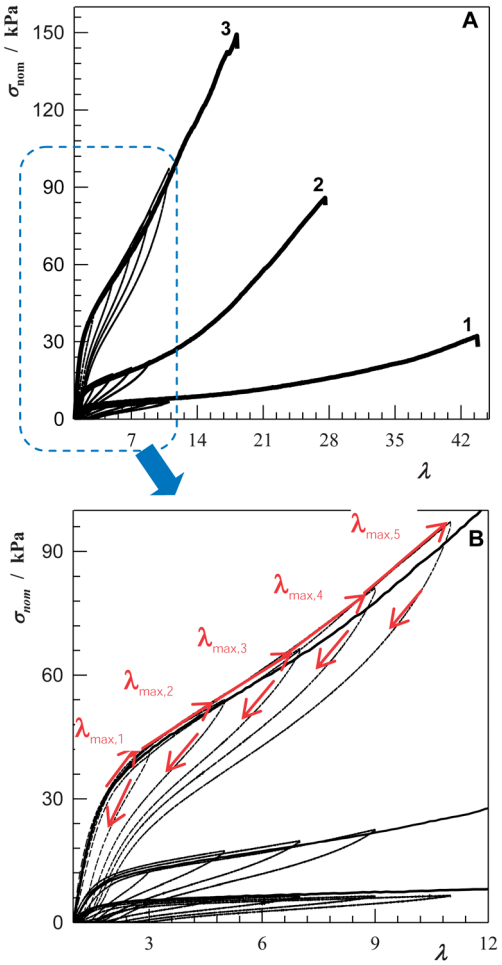

Fig. 2 (A) Stress–strain curves of the gels formed at $C_0 = 15$ (1), 20 (2), and 30 w/v% AAc (3). The dashed rectangular area shows the region of cyclic elongation tests. (B) 5 successive loading/unloading cycles for different values of λ_{max}. The waiting time between cycles = 10 min.

samples to a maximum stain $\lambda_{max,1}$ and then unloading. After a waiting time of 10 min, the samples were again loaded and elongated to an increasing maximum strain $\lambda_{max,2}$ and unloaded. These successive tensile cycles were carried out five times up to $\lambda_{max,5}$ of around 10, as illustrated in Fig. 2B by the red arrows. We found that, for all the gel samples, the n^{th} loading curve is always overlapped by the $(n-1)^{th}$ loading curve over the whole range of $\lambda_{max,n}$. This reveals that no permanent damage occurs during the deformation of the hydrogels up to about 1000% elongation and the bonds broken during elongation are reformed after a waiting time of 10 min. This behavior is completely different from that of double-network hydrogels where the first network is irreversibly broken during loading,[44,45] so that the second loading curve follows the first unloading curve up to $\lambda_{max,1}$. However, it is typical for self-healing gels formed by reversible cross-links.[29,30]

In Fig. 3A, the energy U_{hys} dissipated during the compression cycle calculated from the area between the loading and unloading curves is plotted against λ_{max}. U_{hys} increases with λ_{max}, *i.e.*, with increasing maximum load (Fig. 2B), and with increasing concentration C_0. The hysteresis energy U_{hys} of the

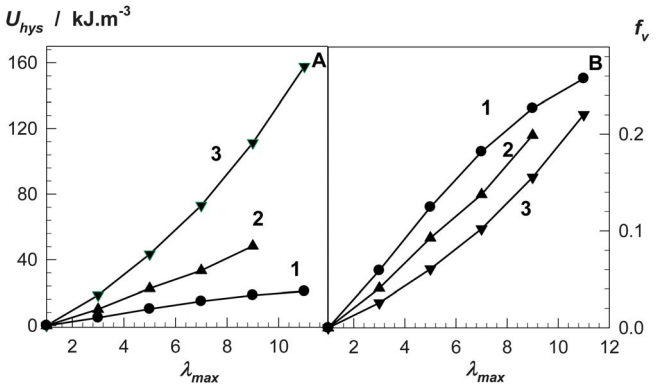

Fig. 3 Hysteresis energy U_{hys} (A) and the fraction f_v of dissociated cross-links during the loading/unloading experiments (B) shown as a function of the maximum elongation ratio λ_{max}. $C_0 = 15$ (1), 20 (2), and 30 w/v% (3).

present gels can be interpreted as the average dissociation energy U_{xl} of a hydrophobic association times the number of associations reversibly broken down during the compression cycle,[44,46] *i.e.*,

$$U_{hys} = U_{xl}\nu_e f_\nu \quad (1)$$

where ν_e is the total number of elastically effective hydrophobic associations, *i.e.*, the cross-link density of the gels, and f_ν is the fraction of associations broken during the loading/unloading cycle. We assume that the energy U_{xl} required for the detachment of the hydrophobe from associations is on the order of 10^2 kJ mol^{-1}.[47,48] The apparent cross-link density ν_e of gels at the experimental time scale was estimated from their moduli E using the equation (we assume a Poisson's ratio of 0.5)[49,50]

$$E = 3(1 - 2/\phi)\nu_e RT(\nu_2^0/\nu_2)^{2/3} \quad (2)$$

where ϕ is the functionality of the cross-links, R is the gas constant, T is the absolute temperature, and ν_2^0 and ν_2 are the volume fractions of physically cross-linked PAAc after the gel preparation and in the equilibrium swollen gel, respectively. The calculation using eqn (2) assumes a phantom network behavior, which is generally appropriate for the transient networks. However, for the present gels formed by hydrophobic associations, since the average aggregation number is large,[51] the cross-link functionality is also large, which will suppress the fluctuations of the cross-links about their mean positions,[52] so that the gels are expected to deform affinely, *i.e.* $(1 - 2/\phi) = 1$. Moreover, because $\nu_2^0 = \nu_2$ for the gels at the state of preparation, eqn (2) reduces to

$$E = 3\nu_e RT \quad (2a)$$

The cross-link densities ν_e of the gels calculated using eqn (2a) are given in the last column of Table 1. The increase of ν_e with C_0 suggests that not only the polymer concentration, but also increasing number of associations acting as effective cross-links contribute to the modulus of gels formed at high concentrations. Using the ν_e values together with eqn (1), we

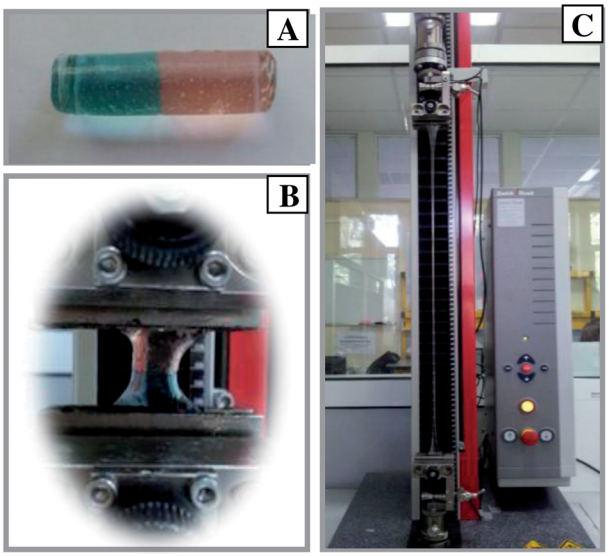

Fig. 4 Photographs of a healed PAAc gel sample formed at $C_0 = 15\%$. The virgin gel samples are colored blue and orange for clarity. (A) Gel sample after healing at 23 ± 2 °C for 30 min. (B and C) The healed gel sample before (B) and during (C) the tensile testing experiments.

estimated the fraction f_v of the associations reversibly broken down during the cyclic tests. In Fig. 3B, the values f_v are plotted against the maximum deformation ratio λ_{max}. Up to about 25% of hydrophobic associations acting as elastically effective cross-links are broken at elongation ratios of about 1000%, but reversibly, if the load is removed, the associations broken reform to form the initial network structure. This suggests that the gels exhibit a strong self-healing behaviour, which will be tested in the following experiments.

As illustrated in Fig. 4A, when the fracture surfaces of a ruptured PAAc gel sample are pressed together, the two pieces merge into a single piece. The reformed joint withstands very large extension ratios before its fracture (Fig. 4B and C). To quantify the healing efficiency, tensile testing experiments were performed using virgin and healed cylindrical gel samples of 5 mm diameter and 6 cm length. The samples were cut in the middle and then the two halves were merged together within a plastic syringe (of the same diameter as the gel sample) by slightly pressing the piston plunger. The healing time was set to 30 min. In preliminary experiments, we observed that the damage created in the gel samples is much better healed by storing them at an elevated temperature. Therefore, in addition to autonomous healing at 23 ± 2 °C, temperature-induced healing tests were carried out at 50 °C and 80 °C. Each experiment was carried out starting from a virgin gel sample.

The solid and dashed curves in Fig. 5A represent typical stress–strain data of virgin and healed gel samples, respectively. Fig. 5B shows the healing efficiency in terms of recovered fracture stress with respect to the virgin sample plotted against the healing temperature. Without an external stimulus, healed hydrogels formed at $C_0 = 15\%$ withstand 10 kPa stress, *i.e.*, autonomous self-healing occurs with 60% efficiency. Increasing C_0 from 15 to 30% also increases the fracture stress of self-healed hydrogels up to 40 kPa while the healing efficiency

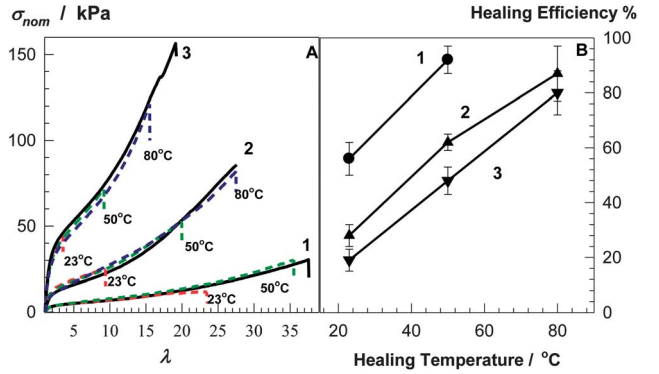

Fig. 5 (A) Stress–strain curves of the virgin (solid curves) and healed gel samples (dashed curves). Healing temperatures are indicated. (B) Healing efficiency of the gel samples shown as a function of the healing temperature. Healing time = 30 min. $C_0 = 15$ (1), 20 (2), and 30 w/v% (3).

decreases to 20%. This is attributed to the simultaneous increase of the cross-link density of hydrogels (Table 1) reducing the chain mobility. Fig. 5 also shows that the healing efficiency significantly increases with increasing temperature. For example, at $C_0 = 30\%$, hydrogels healed at 23 °C fail upon application of 42 ± 5 kPa stress whereas those healed at 80 °C withstand more than 120 kPa stress. All the hydrogel samples self-heal with at least 80% efficiency at 80 °C.

To understand the underlying mechanism of temperature-triggered healing in PAAc hydrogels, we monitored the dynamic moduli of gels as a function of temperature. Fig. 6 shows G', G'' and tan δ of the hydrogel formed at $C_0 = 15$ w/v% plotted against the temperature. Both moduli of the gel sample rapidly decrease as the temperature increases, indicating that the gel becomes weak with rising temperature. Similar results were also obtained for the gels formed at $C_0 = 20$ and 30 w/v% (Fig. S4†). The decrease of the dynamic moduli upon increase of temperature was already observed in semi-dilute solutions of hydrophobically modified PAAms.[33,53] This behavior can be ascribed to increased solubility of hydrophobic moieties in aqueous solutions leading to a decrease in the association degree of polymers.[33] Thus, increasing ability of the hydrogels to self-heal at a high temperature is due to the simultaneous increase of the chain mobility so that the polymer chains on the two cut

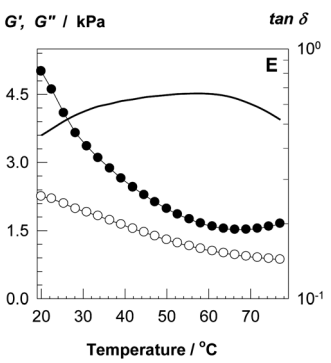

Fig. 6 G' (●), G'' (○) and tan δ (lines) of PAAc hydrogels shown as a function of temperature. $\omega = 6.28$ rad s^{-1}. $\gamma_o = 0.01$. $C_0 = 15$ w/v% AAc.

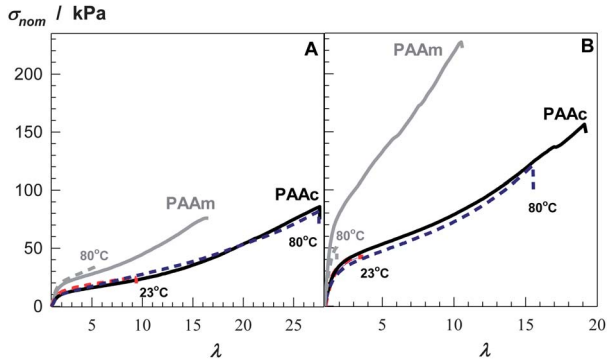

Fig. 7 Stress–strain curves of the virgin (solid curves) and healed gel samples (dashed curves). Healing temperatures are indicated. Results of physical PAAc gels are compared with those for PAAm gels (gray curves). $C_0 = 20$ (A) and 30 w/v% (B).

surfaces can easily diffuse from one side to the other and the hydrophobes across the ruptured interface become more accessible to each other.

For the present hydrogels consisting of hydrophobically modified PAAc network chains, both hydrophobic associations and hydrogen bonding interactions may contribute to their self-healing behaviour. Since the initial pH of the gelation solution was 1.5, the carboxyl groups in gels are mostly protonated which allows them to form hydrogen bonds with other carboxyl groups. To highlight the effect of the PAAc backbone, PAAm hydrogels with 2 mol% C18 were prepared under identical conditions. Fig. 7A and B compare stress–strain curves of virgin and healed PAAm and PAAc hydrogel samples formed at $C_0 = 20$ and 30%, respectively. As compared to PAAc hydrogels, PAAm gels exhibit a reduced ability to self-heal over all the temperatures. For example, the PAAm hydrogel cannot repair itself at 23 °C if the concentration C_0 is 30%, while the PAAc gel healed at the same temperature withstands more than 40 kPa stress. The fracture stress of the hydrogels formed at $C_0 = 30\%$ and healed at 80 °C is 50 and 112 kPa for PAAm and PAAc gels, respectively. We attribute the stronger healing in the PAAc backbone to the cooperative hydrogen bonding between the carboxyl groups stabilizing the hydrophobic domains.

To confirm the contribution of intermolecular hydrogen bonds to the healing process in PAAc gels, we immersed the cut surfaces of the gel samples formed at $C_0 = 20\%$ in a 30% urea solution for 1 min, which is known to disrupt hydrogen bonds. The immersion resulted in a decrease of the healing efficiency from 28 ± 4 to 18 ± 3% at 23 °C (Fig. S5†). This supports our hypothesis that the observed improvement in the self-healing performance of PAAc hydrogels is mediated through hydrogen bonding. Thus, when a PAAc hydrogel sample is cut into two pieces, the broken hydrophobic associations on the cut surfaces reform over time when the cut surfaces are brought into contact while the cooperative hydrogen bonding stabilizes these associations.

Conclusions

Micellar copolymerization of AAc with 2 mol% C18 in the solutions of worm-like SDS micelles produces physical PAAc hydrogels with remarkable properties. The gels exhibit time-dependent dynamic moduli, high modulus (6–53 kPa), high fracture stress (41–173 kPa), high elongation ratios at break (1800–5000%), and self-healing, as evidenced by rheological and mechanical measurements. As the polymer concentration is increased, both the lifetime of hydrophobic associations and the mechanical strength of gels increase while the elongation ratio at break decreases. As compared to PAAm gels formed under identical conditions, the present hydrogels exhibit a much stronger self-healing effect, which is attributed to the cooperative hydrogen bonding between the carboxyl groups stabilizing the hydrophobic domains. The efficiency of self-healing significantly increases with increasing temperature due to the weakening of hydrophobic associations.

Acknowledgements

This work was supported by the Scientific and Technical Research Council of Turkey (TUBITAK), TBAG–109T646. O. O. thanks the Turkish Academy of Sciences (TUBA) for the partial support.

Notes and references

1 P. Fratzl, *J. R. Soc., Interface*, 2007, **4**, 637–642.
2 V. Amendola and M. Meneghetti, *Nanoscale*, 2009, **1**, 74–88.
3 A. R. Hamilton, N. R. Sottos and S. R. White, *Adv. Mater.*, 2010, **22**, 5159–5163.
4 G. E. Fantner, E. Oroudjev, G. Schitter, L. S. Golde, P. Thurner, M. M. Finch, P. Turner, T. Gutsmann, D. E. Morse, H. Hansma and P. K. Hansma, *Biophys. J.*, 2006, **90**, 1411–1418.
5 A. Phadke, C. Zhang, B. Arman, C.-C. Hsu, R. A. Mashelkar, A. K. Lele, M. J. Tauber, G. Arya and S. Varghese, *Proc. Natl. Acad. Sci. U. S. A.*, 2012, **109**, 4383–4388.
6 H. Zhang, H. Xia and Y. Zhao, *ACS Macro Lett.*, 2012, **1**, 1233–1236.
7 J. Cui and A. del Campo, *Chem. Commun.*, 2012, **48**, 9302–9304.
8 J. Liu, G. Song, C. He and H. Wang, *Macromol. Rapid Commun.*, 2013, **34**, 1002–1007.
9 K. Haraguchi, K. Uyama and H. Tanimoto, *Macromol. Rapid Commun.*, 2011, **32**, 1253–1258.
10 A. B. South and L. A. Lyon, *Angew. Chem., Int. Ed.*, 2010, **49**, 767–771.
11 Q. Wang, J. L. Mynar, M. Yoshida, E. Lee, M. Lee, K. Okura, K. Kinbara and T. Aida, *Nature*, 2010, **463**, 339–343.
12 J.-Y. Sun, X. Zhao, W. R. K. Illeperuma, O. Chaudhuri, K. H. Oh, D. J. Money, J. J. Vlassak and Z. Suo, *Nature*, 2012, **489**, 133–136.
13 C. T. S. W. P. Foo, J. S. Lee, W. Mulyasasmita, A. Parisi-Amon and S. C. Heilshorn, *Proc. Natl. Acad. Sci. U. S. A.*, 2009, **106**, 22067–22072.
14 E. A. Appel, F. Biedermann, U. Rauwald, S. T. Jones, J. M. Zayed and O. A. Scherman, *J. Am. Chem. Soc.*, 2010, **132**, 14251–14260.

15 P. J. Skrzeszewska, J. Sprakel, F. A. Wolf, R. Fokkink, M. A. C. Stuart and J. van de Gucht, *Macromolecules*, 2010, **43**, 3542–3548.
16 N. Holten-Andersen, M. J. Harrington, H. Birkedal, B. P. Lee, P. B. Messersmith, K. Y. C. Lee and J. H. Waite, *Proc. Natl. Acad. Sci. U. S. A.*, 2011, **108**, 2651–2655.
17 Z. Shafiq, J. Cui, L. Pastor-Perez, V. San Miguel, R. A. Gropeanu, C. Serrano and A. del Campo, *Angew. Chem.*, 2012, **124**, 4408–4411.
18 Y. Xu, Q. Wu, Y. Sun, H. Bai and G. Shi, *ACS Nano*, 2010, **4**, 7358–7362.
19 F. Liu, F. Li, G. Deng, Y. Chen, B. Zhang, J. Zhang and C.-Y. Liu, *Macromolecules*, 2012, **45**, 1636–1645.
20 G. Deng, C. Tang, F. Li, H. Jiang and Y. Chen, *Macromolecules*, 2010, **43**, 1191–1194.
21 Y. Zhang, L. Tao, S. Li and Y. Wei, *Biomacromolecules*, 2011, **12**, 2894–2901.
22 L. He, D. E. Fullenkamp, J. G. Rivera and P. B. Messersmith, *Chem. Commun.*, 2011, **47**, 7497–7499.
23 P. Froimowicz, D. Klinger and K. Landfester, *Chem.–Eur. J.*, 2011, **17**, 12465–12475.
24 S. B. Quint and C. Pacholski, *Soft Matter*, 2011, **7**, 3735–3738.
25 D. C. Tuncaboylu, M. Sari, W. Oppermann and O. Okay, *Macromolecules*, 2011, **44**, 4997–5005.
26 J. Hao and R. A. Weiss, *Macromolecules*, 2011, **44**, 9390–9398.
27 X. Hao, H. Liu, Y. Xie, C. Fang and H. Yang, *Colloid Polym. Sci.*, 2013, **291**, 1749–1758.
28 G. Jiang, C. Liu, X. Liu, G. Zhang, M. Yang, Q. Chen and F. Liu, *J. Macromol. Sci., Part A: Pure Appl. Chem.*, 2010, **47**, 335–342.
29 D. C. Tuncaboylu, M. Sahin, A. Argun, W. Oppermann and O. Okay, *Macromolecules*, 2012, **45**, 1991–2000.
30 D. C. Tuncaboylu, A. Argun, M. Sahin, M. Sari and O. Okay, *Polymer*, 2012, **53**, 5513–5522.
31 G. Akay, A. Hassan-Raesi, D. C. Tuncaboylu, N. Orakdogen, S. Abdurrahmanoglu, W. Oppermann and O. Okay, *Soft Matter*, 2013, **9**, 2254–2261.
32 F. Candau and J. Selb, *Adv. Colloid Interface Sci.*, 1999, **79**, 149–172.
33 E. Volpert, J. Selb and F. Candau, *Polymer*, 1998, **39**, 1025–1033.
34 A. Hill, F. Candau and J. Selb, *Macromolecules*, 1993, **26**, 4521–4532.
35 E. J. Regalado, J. Selb and F. Candau, *Macromolecules*, 1999, **32**, 8580–8588.
36 F. Candau, E. J. Regalado and J. Selb, *Macromolecules*, 1998, **31**, 5550–5552.
37 P. Kujawa, A. Audibert-Hayet, J. Selb and F. Candau, *J. Polym. Sci., Part B: Polym. Phys.*, 2004, **42**, 1640–1655.
38 P. Kujawa, A. Audibert-Hayet, J. Selb and F. Candau, *Macromolecules*, 2006, **39**, 384–392.
39 U. P. Schroder and W. Oppermann, Properties of polyelectrolyte gels, in *Physical Properties of Polymeric Gels*, ed. J. P. Cohen Addad, Wiley, NY, 1996, pp. 19–38.
40 G. Miquelard-Garnier, C. Creton and D. Hourdet, *Soft Matter*, 2008, **4**, 1011–1023.
41 G. Miquelard-Garnier, D. Hourdet and C. Creton, *Polymer*, 2009, **50**, 481–490.
42 C. Bilici and O. Okay, *Macromolecules*, 2013, **46**, 3125–3131.
43 T. Miyazaki, K. Yamaoka, J. Gong and Y. Osada, *Macromol. Rapid Commun.*, 2002, **23**, 447–455.
44 R. E. Webber, C. Creton, H. R. Brown and J. P. Gong, *Macromolecules*, 2007, **40**, 2919–2927.
45 H. R. Brown, *Macromolecules*, 2007, **40**, 3815–3818.
46 G. J. Lake and A. G. Thomas, *Proc. R. Soc. London, Ser. A*, 1967, **300**, 108–119.
47 T. Annable, R. Buscall, R. Ettelaie and D. Whittlestone, *J. Rheol.*, 1993, **37**, 695–726.
48 W. K. Ng, K. C. Tam and R. D. Jenkins, *J. Rheol.*, 2000, **44**, 137–147.
49 P. J. Flory, *Principles of Polymer Chemistry*, Cornell University Press, Ithaca, NY, 1953.
50 L. R. G. Treloar, *The Physics of Rubber Elasticity*, University Press, Oxford, 1975.
51 Y. A. Shashkina, Y. D. Zaroslov, V. A. Smirnov, O. E. Philippova, A. R. Khokhlov, T. A. Pryakhina and N. A. Churochkina, *Polymer*, 2003, **44**, 2289.
52 J. E. Mark and B. Erman, *Rubberlike Elasticity. A Molecular Primer*, Cambridge University Press, Cambridge, UK, 2007.
53 S. Biggs, J. Selb and F. Candau, *Polymer*, 1993, **34**, 580–591.